# Relationships between tensile strength, morphology and crystallinity of treated kenaf bast fibers

H. Sosiati, Ar Rohim, Ma`arif, K. Triyana, and Harsojo

## Additional information on AIP Conf. Proc.

# Relationships between Tensile Strength, Morphology and Crystallinity of Treated Kenaf Bast Fibers

H. Sosiati[1,2*], Ar Rohim[3], Ma`arif[3], K. Triyana[1,3] and Harsojo[1,3]

[1] *Nanomaterials Research Group, Integrated Research and Testing Laboratory (LPPT),*
*Gadjah Mada University, Yogyakarta 55281, Indonesia*
[2] *The Graduate School, Gadjah Mada University, Yogyakarta 55281, Indonesia*
[3] *Department of Physics, Faculty of Mathematics and Natural Sciences,*
*Gadjah Mada University, Yogyakarta 55281, Indonesia*
**hsosiati@ugm.ac.id*

**Abstract.** Surface treatments on kenaf bast fibers were carried out with steam, alkali and a combination of steam-alkali. To verify and gain an understanding of their inter-relationship, tensile strength, surface morphology and crystallinity of treated and raw fibers were characterized. Tensile strength of fibers was measured with a universal tensile machine (UTM), crystallinity was estimated using X-ray diffraction (XRD) and Fourier transformation infrared (FTIR) spectroscopy, and surface morphology was examined by scanning electron microscopy (SEM). Tensile strength of the treated fibers was higher than that of the raw fiber. Tensile strength increased after steam treatment and was further improved by alkali treatment, but slightly reduced after steam treatment followed by alkalization. Increase of concentration of alkali tended to increase tensile strength. Differences in tensile strength of the treated fibers are discussed in relation to the changes in surface morphology and crystallinity. Understanding of these relationships may provide direction towards the goal of producing better performance of natural fiber composites.

**Keywords:** kenaf bast fiber, surface treatment, tensile strength, crystallinity, morphology
**PACS:** 81.05.Lg, 81.65.-b, 81.40.Lm, 81.40-z

## INTRODUCTION

The manufacturing of natural fiber-based materials is expected to provide one option for meeting the need for environmentally friendly alternatives to those currently used. The end of life vehicle (ELV) directive in Europe states, that by 2015 vehicles must be constructed of 95% recyclable materials with 85% recoverable through reuse or mechanical recycling and 10% through thermal recycling [1]. Advantageous properties of natural fibers including low cost and weight, environmentally safe and biodegradability, offer the potential for developing green fiber polymer composite technologies. For instance, kenaf fiber-based polymer composites are known to have potential in various applications such as boards, and automobile bodies and interiors [2, 3].

The hydrophilic nature of the fibers makes them incompatible for interacting with the hydrophobic nature of the polymeric matrix. This is the main problem in fabricating natural fiber composite [4]. To increase interfacial adhesion and also compatibility between the fibers (as fillers) and the polymeric matrix, surface treatment on the fiber is required. Various treatments of the fibers to improve their properties and the corresponding composite have been reported including alkali treatment, steam-explosion at high pressure and a combined steam-alkali treatment [5-7].

At large scales, use of alkali may be environmentally unsafe. Although steam treatment is simple in principle and there is no environmental effect but steaming at high pressure consumes energy and is high cost. Single-fiber bonding is stronger following alkali treatment than steam-explosion [8]. However, steam treatment improves the crystallinity of the fiber [6, 7] and its mechanical strength [9]. The influence of surface treatments on the fiber properties including those of kenaf fiber is not fully understood.

In this study, we characterized the properties (tensile strength, morphology, crystallinity) of the treated (steam, alkali, steam-alkali) kenaf fibers and compared them with those of raw fiber in order to verify and gain an understanding their relationships.

# EXPERIMENTAL

Kenaf fiber variety KR-11 was obtained from Ballitas, Malang, East-Java, Indonesia. Fibers of approximately 3-4 m length and 100 μm average diameter were cut into ca. 5 cm lengths and dried in an oven at 70ºC for 30 min. Raw-kenaf (RK) fibers were treated with alkali solution (NaOH), steam and a combination of steam–alkali (Table 1). Detailed treatments have been described elsewhere [10].

**TABLE 1.** Treatment of kenaf

| Sample | Treatment | |
|---|---|---|
| | Steam (1.8 Bar) | NaOH (100ºC, 1h) |
| RK | x | x |
| S3 | x | 3 g/L |
| S10 | x | 10 g/L |
| ST20 | 20 min | x |
| ST10-S10 | 10 min | 10 g/L |

The tensile test of raw and treated fibers was done with a universal tensile machine (UTM, Torsee AMU-5-DE) and the tensile test specimen was prepared by referring to ASTM D-3379. The tested fibers were embedded in the resin and mechanically polished to measure the average diameter of each fiber from its cross-sectional area. Five different fibers were measured for each treated fiber. The tensile strength of the fiber was determined based on the following equation,

$$\sigma = F/A \qquad (1)$$

where σ is tensile strength ($N/mm^2$), F is force at failure (N) and A is the surface area of the fiber (mm).

Fiber morphology of raw-kenaf and the treated fibers were examined by scanning electron microscopy (SEM, INSPEX S50-FEI). XRD (XRD, X`Pert Pro, PANalytical) was employed to confirm crystalline cellulose in the fiber from the XRD profile and to estimate the X-ray crystallinity index (CI) of the fiber using the XRD software package for the XRD converter. CI (%) was calculated from the ratio of the area of all crystalline peaks (at 2θ between 10-40º) to the total area including non-crystalline area as follows [11],

$$CI = \frac{I_{cr\ peak1} + I_{cr\ peak2} + I_{cr\ peak3}}{I_{cr\ peak1} + I_{cr\ peak2} + I_{cr\ peak3} + I_{non-cr}} \times 100\% \quad (2)$$

where, $I_{cr\ peak1,\ 2,\ 3}$ are the crystalline peak areas 1, 2 and 3 in the XRD patterns corresponding to cellulose crystalline reflections -111 (peak1), 002 (peak2) and -231 (peak3) (PDF # 030289). $I_{non-cr}$ is the area under the non-crystalline peak of the cellulose diffraction pattern.

Fourier transformation infrared (FTIR, Shimadzu) spectroscopy was used to identify the functional group attributed to cellulose, lignin and hemicelluloses contained in all fiber specimens especially in the range of 1700-500 $cm^{-1}$, and to estimate the IR CI of cellulose from the ratio of absorbance intensity at 1427 and 895 $cm^{-1}$ which are respectively assigned to $CH_2$ bending mode [12, 13] and deformation of anomeric CH [14]: i.e. ($A_{1427}/A_{895}$).

# RESULTS AND DISCUSSION

## Tensile Strength

Tensile strength of the treated fibers was higher than that of the raw fiber (Fig. 1). It slightly increased after steaming for 20 min (specimen ST20) and was further improved by alkali treatment in concentrations of 3g/L and 10g/L (specimens S3 and S10, Table 1), then somewhat decreased after steaming which was followed by alkali treatment (specimen ST10-S10, Table 1). Interestingly, a short period of steaming and alkali treatment with relatively low concentration changed fiber strength. The changes observed can be attributed to the differences in surface morphologies and the crystallinity of fibers.
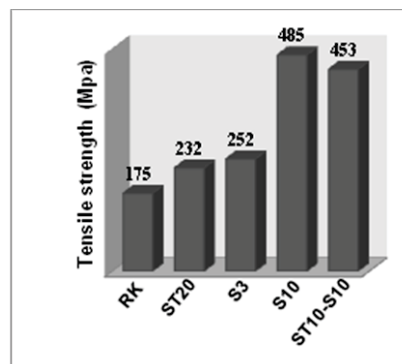


**FIGURE 1**. Tensile strength of raw fiber and the treated kenaf fibers.

## Surface Morphology

The surface morphology of a single raw kenaf fiber (RK) (φ: ~100 μm) shows parallel lines which look like fiber segments (Fig. 2a). A single fiber consists of cellulose microfibrils embedded in the soft matrix of the amorphous non-cellulosic constituents; lignin and hemicelluloses [15]. Lignin and hemicelluloses were apparently broken after

steaming, and the cellulose microfibrils with average diameter of 20 μm exposed on the fiber surface (Fig. 2b). Fine particles in bright contrast distributed on the fiber surface (see arrows) are interpreted as the
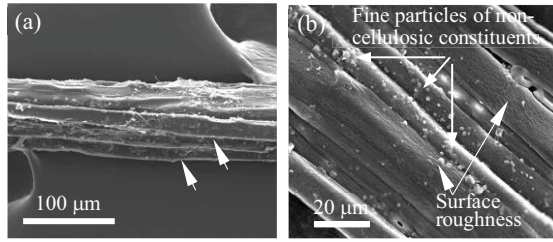


FIGURE 2. SEM images of raw kenaf fiber (a) and steam treated fiber for 20 min, specimen ST20 (b).

non-cellulosic (lignin and hemicelluloses), because lignin is insoluble in steam or hot water and hemicelluloses are destroyed rapidly by heating [16]. Some fibers also display high surface roughness (see arrows). Lignin is totally amorphous and hydrophobic in nature but hemicelluloses are very hydrophilic [17]. Thus, steam treatment tended to make the fiber a little more hydrophobic.

Fig. 3a and b exhibit SEM images of the alkali treated fiber, specimens S3 and S10, respectively. Their morphologies are similar and partly free from non-cellulosic constituents with average fiber diameter of about 15 μm. Small holes observed on fiber surface (Fig. 3a, see arrows) are probably formed because the strong electron beam hit the area where the fiber coating might be thinner than in the surrounding areas. Fiber bundles had partly decomposed to be individual fibers with relatively high surface roughness (see arrows). The remaining lignin is clearly depicted in Fig. 3b (see arrows).
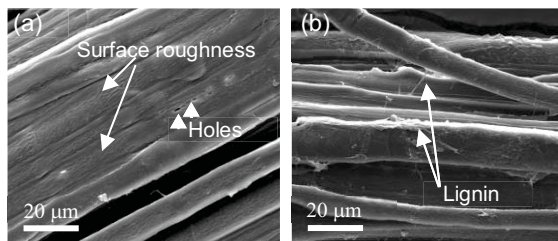


FIGURE 3. SEM images of alkali treated fibers with 3g/L NaOH, specimen S3 (a) and with 10g/L NaOH, specimen S10 (b).

During alkali treatment hydroxyl group on the fiber surface interacted with NaOH to form alkali cellulose as follows [17].

$$\text{Fiber-OH} + \text{Na-OH} \rightarrow \text{Fiber-ONa}^+ + \text{H}_2\text{O} \quad (3)$$

This interaction removed the hydrogen bonding in the network structure and increased the amount of cellulose microfibrils exposed on the fiber surface. As alkali concentration increased the amount of extracted cellulose microfibrils also increased. In this case, hemicelluloses are soluble in alkali and lignin is soluble in hot alkali, whereas cellulose is resistant to strong alkali and oxidizing agents [17].

It is suggested that in the steam treatment followed by alkali treatment (specimen ST10-S10, Table 1) hemicelluloses are first destroyed by steaming followed by dissolution of lignin and hemicelluloses by alkali. Careful observation of steam-alkali treated fiber indicated that surface morphology of this specimen is freer from lignin and higher in surface roughness than specimen S3 and S10. Figs. 5a and b represent the fiber morphology of a relatively clear area and an area with slightly retained lignin, respectively, of specimen ST10-S10. The average diameter of this fiber was relatively similar to those of S3 and S10 suggesting that short steaming prior to alkali treatment did not have a significant effect on the decomposition of the fibers.
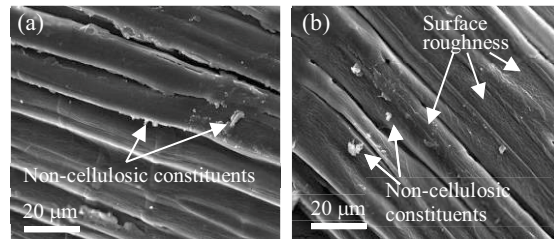


FIGURE 4. SEM images of steam-alkali treated fibers (specimen ST10-S10) showing higher surface roughness in (b) than (a).

## Crystallinity

XRD profiles of raw fiber and the treated fibers (Fig. 5) show almost similar patterns; peak 1, peak 2 and peak 3 positioned at 2θ around 16.493º ($I_{-111}$ lattice reflection), 22.841º ($I_{002}$ lattice reflection) and
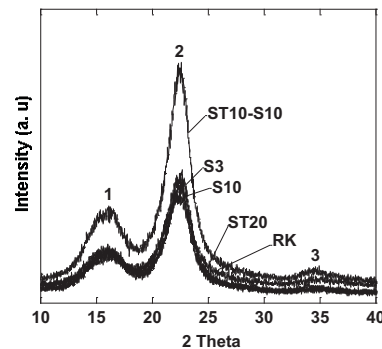


FIGURE 5. XRD profiles of raw kenaf fiber (RK) and the treated fibers (ST20, S3, S10 and ST10-S10).

44

34.602º ($I_{-231}$ lattice reflection), respectively (native cellulose, PDF # 030289). These results confirmed that microfibrils observed after treating with steam, alkali and a combination of steam-alkali mostly crystalline cellulose microfibrils. According to equation (2) XRD *CI* of raw fiber and the treated fibers are estimated to be 0.34 (RK), 0.40 (ST20), 0.43 (S3), 0.46 (S10) and 0.45 (ST10-S10). The trend of changes in XRD *CI* of the fibers after treating with steam, alkali and a combination of steam-alkali treatments is consistent with that in tensile strength. This suggests that the higher the volume fraction of crystalline cellulose formed within the fiber, the higher the fiber strength. In addition, an inhomogeneous distribution of crystalline cellulose in the fiber is possible. This is reflected in the increase of XRD *CI* of specimens S3 and S10 but is not in accordance with dramatic increase of tensile strength of the same specimens.

FTIR spectra obtained from all specimens (RK, S20, S3, S10 and ST10-S10) (Fig. 6) were used to confirm the presence of cellulose, lignin and hemicelluloses especially within the wave number 1800-500 $cm^{-1}$. Absorption peaks at 1720-1728 $cm^{-1}$ and 1242-1249 $cm^{-1}$ for specimens RK and ST20 are assigned to C=O stretching of the acetyl group in hemicelluloses and C-O stretching of the aryl group in lignin [18]. These two peaks had disappeared in
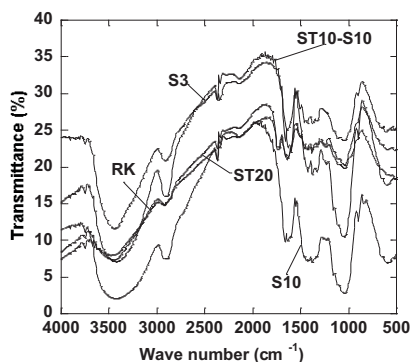


**FIGURE 6**. FTIR spectra of raw kenaf fiber (RK) and the treated fibers (ST20, S3, S10 and ST10-S10).

FTIR spectra for other treated specimens (S3, S10 and ST10-S10). The peak at 1635 $cm^{-1}$ for RK, ST20 and S3 represents absorbed water [19]. The small peak at 1427 $cm^{-1}$ for the treated specimens corresponds to $CH_2$ symmetric bending that is known as the crytallinity band. Peaks observed between 1373-1381 $cm^{-1}$ for all specimens are associated with weak C-O stretching [20, 21] and those around 1327-1334 $cm^{-1}$ are attributed to S ring stretching in lignin [22]. Absorbance at around 898-895 $cm^{-1}$ for the treated specimens is assigned to C-O-C stretching of glycoside bonds which is symmetric in polymorphic

and designed as an amorphous absorption band [12]. *CI* of cellulose from FTIR spectra could only be estimated for the treated specimens according to the ratio of ($A_{1427}/A_{895}$): i.e. 0.93 for S3, 1.56 for S10 and 1.41 for ST10-S10, because no absorption peaks at 1427 and 895 $cm^{-1}$ for specimen RK and ST20 were identified. It might be affected by hydrogen bonding in the range of 3500 to 3000 $cm^{-1}$ for specimens RK and ST20 (Fig.7) reveal in similar shape and intensity which are different from three other specimens [23]. Change in IR *CI* has similar trend to XRD *CI* and alteration of tensile strength.

## Relationship between Tensile Strength, Morphology and Crystallinity

The differences observed in tensile strength, morphology and crystallinity of the treated fibers compared to raw fiber can be understood from the structure of the fiber. In principle, the structure plant fiber including kenaf consists of two layers of cell walls. The primarily wall mostly contains disorderly networks of crystalline cellulose microfibrils. The secondary wall ($S_1$, $S_2$ and $S_3$) comprises of three layers containing helically arranged crystalline cellulose microfibrils. $S_2$ is the thickest one which determines the strength of fiber [24].

We have considered that surface treatment changed disordering atomic structure of cellulose to be ordering atomic structure through crystallization of the cellulose. The type of or conditions during surface treatment play an important role in the expression of this crystallization. For the surface treatments used in this study, it is evident that steam treatment (ST20) was insufficient to reorder the atomic structure of the cellulose as there was no removal of lignin and hemicelluloses resulting in only a slight increase of *CI*, tensile strength and the amount of cellulose microfibrils exposed on the fiber surface. The alkali treated fiber (S10) had the highest *CI* and tensile strength, and also high surface roughness, suggesting a close relationship between tensile strength, crystallinity and surface morphology of the fiber. An ideal surface treatment would produce fiber properties that were most suitable for producing the composite.

## CONCLUSIONS

By using SEM, XRD and FTIR spectroscopy, we have verified and now better understand the relationship between the properties (tensile strength, surface morphology and crystallinity) of kenaf fiber following surface treatments of steam, alkali and a combination of steam-alkali. Removal of hydrogen

45

bonding in the network structure resulted in high level exposure of cellulose microfibrils on the fiber surface with high surface roughness. This reflected high crystallinity providing an improvement of fiber strength. Crystallinity correlates with fiber properties. Understanding the relationship between these properties make a useful contribution to producing better performance of natural fiber composites.

## ACKNOWLEDGMENTS

## REFERENCES

1. T. Peijs, *Materials Today*, **6**(4), 30-35 (2003).
2. J. Holbery and D. Houston, *JOM* **32**, 80-86 (2006).
3. M. Zampaloni, F. Pourboghrat, S. A. Yankovich, B. N. Rodgers, J. Moore, L. T. Drzal, A. K. Mohanty and M. Misra, *Composites Part A* **38**, 1569-1580 (2007).
4. I. S. Aji, S. M. Sapuan, E. S. Zainudin and K. Abdan, *International Journal of Mech. Mater. Eng.* **4**, 239-248 (2009).
5. Y. Cao, S. Sakamoto, K. Goda, *Proc. of 16th Int. Conf. on Composite Materials*, Japan, 1-4 (2007).
6. M. M. Ibrahim, F. A. Agblevor and W. K. El Zawawy, *BioResources* **5**, 397-418 (2010).
7. S. S. Munawar, K. Unemura, F. Tanaka and S. Kawai, *J. Wood Sci.* **53**, 481-485 (2007).
8. T. P. Nguyen, T. Fuji, B. Chuong and K. Okubo, *J. Mater. Sci. Res.* **1**(1), 144-155 (2012).
9. R. M. Rowell and H. P. Stout, "Jute and Kenaf", in *Handbook of Fiber Chemistry*, edited by M. Lewin, New York: Marcell Dekker, 2007, pp. 415-416.
10. H. Sosiati, Harsojo, Soekrisno, R. Widyorini, D.A. Wijayanti and K. Triyana, *Proc. of 3th Jogja Int. Physics Conf.*, Indonesia, 18-19 (2012).
11. R. Ibbet, D. Domvoglou and D. A. S. Phillips, *Cellulose* **15**, 241-254 (2008).
12. D. Ciolacu, F. Ciolacu and V. I. Popa, *Cellulose Chem. Technol*. **45**(1-2), 13-21 (2011).
13. C. Y. Liang and R. H. Marchessault, *J. Polym. Sci.* **37**, 385-395 (1959).
14. J. Blackwell, P. D. Vasko and J. L. Koenig, *J. Appl. Phys.* **41**, 4375-4379 (1970).
15. G. Siqueria, J. Bras and A. Dufresne, *Polymers* **2**, 728-765 (2010).
16. H. K. Eslam, S. E. Saieh and M. Rajabi, *Australian Journal of Basic and Applied Sciences* **5**(6), 1143-1150 (2011).
17. M. J. John and R. D. Anandjiwala, *Polymer Composites* **29**(2), 187-207 (2008).
18. M. Troedec, D. Sedan, C. Peyratout, J. Bonnet, A. Smith, R. Guinebretiere, V. Gloaguen and P. Krausz, *Composites Part A* **39**, 514-522 (2008).
19. N. Nosbi, H. M. Akil, Z. A. M. Ishak and A. Abu Bakar, *BioResources* **6**(2), 950-960 (2011).
20. P. Yu, H. Block, Z. Niu and K. Doiron, *J. Synchrotron Radiation* **14**, 382-390 (2007).
21. F. Xu, J. X. Sun, Z. C. Geng, C. F. Liu, J. L. Ren, R. C. Sun, P. Fowler and M. S. Baird, *Carbohydrate Polymers* **67**, 56-65 (2007).
22. E. Sjöström, *Wood Chemistry Fundamental and Applications*, San Diego: Academic Press, 1981, pp. 73-83.
23. C. P. S. Hsu, *Handbook of Instrumental Techniques for Analytical Chemistry*, New Jersey: Prentice-Hall, 1997, pp. 266-270.
24. M. M. Kabir, H. Wang, K. T. Lau and F. Cardona, *Composites Part B* **43**(7), 2883-2892 (2012).